

Capacity Regions of Gaussian Multiple-access Channels with Intersymbol Interference

ROGER S. CHENG and SERGIO VERDÚ
Department of Electrical Engineering
Princeton University
Princeton, NJ 08544

Abstract

Memoryless channels have occupied the center stage in multiuser information theory. Not until recently have their counterparts with memory started to receive well deserved attention. In this paper, we find the capacity region of a Gaussian multiple-access channel (MAC) with intersymbol interference (ISI) where the input vectors of the users pass through their corresponding linear systems and then superimpose (or, equivalently pass through a linear system with multiple vector inputs) before being corrupted by additive colored Gaussian noise vector process. This can be viewed as either a generalization of the classical Gaussian MAC to channel with memory or the generalization of the single-user intersymbol interference channel to the multi-user case.

In the univariate case where the inputs and output are real numbers, the optimal power spectral densities for the users can be obtained via two concepts: the water-filling argument and successive decoding (decode one user's information treating the other as noise, subtract, and then decode the other user's information.) In contrast to the classical Gaussian MAC, the capacity region of this channel with memory is, in general, not a pentagon unless the transfer functions for both users are identical. When the energy of the transfer functions are fixed, ISI always decreases the single-user capacity. However, it turns out that ISI may increase the total capacity of a two-user channel.

I Introduction

Information theoretical limits of memoryless channels have been studied extensively since Shannon in 1948. The capacities and the capacity regions of single-user and multi-user memoryless channels were found by Shannon [1] and Alhuswede [2] (see also [3, 4]), respectively. However, channels with memory did not receive as much attention as its memoryless counterparts. This is partly due to the fact that the single-letter characterization [5] for the capacities of channels with memory do not exist. Only a limiting expression [6] is known for the capacities of single-user channels with memory and a not uncommon misconception is to discuss limiting expressions for capacity as

uncomputable. The classical example where limiting expressions can be not only readily computed but lead to a celebrated solution is the Gaussian single-user channel with intersymbol interference (ISI) ([7, 8, 9], see also [10]).

In a recent paper by Verdú [11], a similar limiting expression for the capacity regions of multiple-access channels with memory is obtained. Such a limiting expression is explicitly evaluated in some channels with memory. In particular, the limiting expression is applied to the asynchronous code-division multiple-access (CDMA) channel (which can be viewed as a multiple-access channel with memory) [12] to obtain its capacity region. In this special case, the capacity region can be evaluated by solving an optimization problem with low computational complexity.

Perhaps the most commonly encountered channels with memory are the intersymbol interference (ISI) Gaussian channels shown in Figure 1. The capacity of a single-user ISI Gaussian channel is usually obtained through a Karhunen-Loève expansion. It decomposes the ISI Gaussian channel into independent parallel memoryless Gaussian channels whose capacities are well known; thereby reducing the problem to one of optimal power allocation into various channels. It is crucial to note that the kernel used in the Karhunen-Loève expansion depends on the ISI coefficients. In the two-user Gaussian channel with ISI, there are two sets of ISI coefficients, one for each users. If they are identical, the traditional procedures can be applied and the capacity regions had been obtained [13, 14]. However, if the sets of ISI coefficients are not the same, a similar decomposition into independent memoryless channels cannot be applied since no kernel can simultaneously decompose the signals from both users. It is plausible that this is the reason why the capacity regions of multi-user ISI Gaussian channels have not been reported yet.

Recently, a new approach to obtain the capacities of Gaussian channels with ISI is proposed ([15], and independently in [12]). This approach enables an orthogonal decomposition of the channel using Discrete Fourier Transform (DFT) which is independent of the ISI coefficients. In this paper, we employ this idea and the limiting expression for the capacity regions of multiple-access channels with memory to obtain the capacity regions of a Gaussian linear multiple-access channels.

We consider a Gaussian linear multiple-access channel as shown in Figure 2, or, equivalently, Figure 3. The only assumptions are that the channel is linear and time-

This work was supported by the Office of Naval Research under Grant N00014-90-J-1734.

invariant with finite-length impulse response, and the noise is stationary and m -dependent (i.e. the autocorrelation function has finite support.) This model is a generalization of the classical multiple-access channel, and includes the Gaussian multiple-access channel with finite ISI and the CDMA channel. In this paper, we find the capacity region of this channel model and use it to obtain the capacity regions of the Gaussian multiple-access ISI channels.

When the inputs and the output are real numbers, the model is a generalization of the classical ISI Gaussian channel to the multi-user case shown in Figure 1. In this case, it turns out that the boundary points of the capacity region are determined by two main ideas: one is akin to the water-filling argument in the single-user ISI channel, and the other involves the idea of successive decoding (decode the first user's information while treating the second user's information as noise and then decode the second user's information) in the classical multiple-access channel.

In Section II, the main theorem giving the capacity region of a Gaussian multiple-access linear vector channel is presented. Then, we specialize the result to the univariate case (inputs and output are real number) in Section III where we come up with a generalization of the water-filling formula to the two-user case. Examples of some simple channels are given to demonstrate how the optimal power spectral densities are obtained by the idea of successive decoding and the water-filling arguments.

II Capacity Region of Gaussian linear MAC

The channel model we consider is a linear multiple-access channel with addition Gaussian noise shown in Figure 2. It is easy to see, by linearity, that the models in Figure 2 and 3 are equivalent and they include, as a special case, the Gaussian multiple-access channel with ISI in Figure 1. From now on, we shall concentrate on the model in Figure 3:

$$\tilde{Z}_i = \sum_{j=0}^m \tilde{G}_j \tilde{U}_{i-j} + \tilde{H}_j \tilde{V}_{i-j} + \tilde{N}_i \quad (1)$$

where \tilde{Z}_i is the output of the channel in \mathbb{R}^r , \tilde{U}_i and \tilde{V}_i are symbols sent by user 1 and 2 in \mathbb{R}^p and \mathbb{R}^q , respectively, and \tilde{N}_i is a zero-mean stationary Gaussian noise vector process with autocorrelation function $\tilde{R}_{i-j} \triangleq E(\tilde{N}_i \tilde{N}_j^T)$. The power constraint requires each codeword of the k^{th} user, $(c_{k0}, \dots, c_{k(N-1)})$, of each (N, M_1, M_2, ϵ) code (for definition, see (e.g. [5])) to satisfy

$$\frac{1}{N} \sum_{i=0}^{N-1} \|c_{ki}\|_2^2 \leq W_k \quad (2)$$

where $\|\cdot\|_2$ denotes the l_2 norm. We assume that both channels have finite-length impulse responses with length n , and the noise process is an m -dependent stationary process (i.e. \tilde{N}_i and \tilde{N}_j are independent for all $|i-j| > m$.) These are crucial assumptions in the proof of our result. However, the causality assumption is introduced for convenience and ease of notation only. The same result follows if the channel is non-causal, provided that the impulse response has finite length.

Since this channel is a special case of a general multiple-access channel with finite memory, we can make use of a result in [11] which gives the capacity region as a limit of the capacity regions, C_N , of a series of N -block channels. Applying that result here and denoting C as the capacity region of the Gaussian linear multiple-access channel, we have

$$C = \text{Closure} \left(\liminf_{N \rightarrow \infty} C_N \right) \quad (3)$$

where

$$C_N = \bigcup_{\substack{\tilde{U}_0^{N-1}, \tilde{V}_0^{N-1}: \\ \sum_{i=0}^{N-1} \text{tr} E(\tilde{U}_i \tilde{U}_i^T) \leq N W_1 \\ \sum_{i=0}^{N-1} \text{tr} E(\tilde{V}_i \tilde{V}_i^T) \leq N W_2}} \left\{ (R_1, R_2) : \begin{array}{l} R_1 \leq \frac{1}{N} \mathbf{I}(\tilde{U}_0^{N-1}, \tilde{V}_0^{N-1} | \tilde{V}_0^{N-1}) \\ R_2 \leq \frac{1}{N} \mathbf{I}(\tilde{V}_0^{N-1}, \tilde{U}_0^{N-1} | \tilde{U}_0^{N-1}) \\ R_1 + R_2 \leq \frac{1}{N} \mathbf{I}(\tilde{U}_0^{N-1}, \tilde{V}_0^{N-1}; \tilde{Y}_0^{N-1}) \end{array} \right\} \quad (4)$$

In (4), \tilde{Y}_0^{N-1} is defined as

$$P_{\tilde{Y}_0^{N-1} | \tilde{U}_0^{N-1}, \tilde{V}_0^{N-1}}(\tilde{y}_0^{N-1} | \tilde{u}_0^{N-1}, \tilde{v}_0^{N-1}) = P(\tilde{y}_0^{t-1} | \tilde{u}_0^{N-1}, \tilde{v}_0^{N-1}) P_{\tilde{Z}_t^{N-1} | \tilde{U}_0^{N-1}, \tilde{V}_0^{N-1}}(\tilde{y}_t^{N-1} | \tilde{u}_0^{N-1}, \tilde{v}_0^{N-1}) \quad (5)$$

where t is the maximum of n , the length of the impulse response, and m , the length of the noise autocorrelation function. As pointed out in [11], the important aspect of this result is that P can be any conditional probability density function. This flexibility allows us to define P appropriately so that the N -block channel becomes

$$\tilde{Y}_0^{N-1} = \tilde{G}_0^{N-1} \otimes \tilde{U}_0^{N-1} + \tilde{H}_0^{N-1} \otimes \tilde{V}_0^{N-1} + \tilde{M}_0^{N-1} \quad (6)$$

where \otimes denotes the circular convolution and \tilde{M}_0^{N-1} are jointly Gaussian with mean zero and $E(\tilde{M}_i \tilde{M}_j) = \tilde{R}_{(i-j)_N}$ where $(\cdot)_N$ denotes the modular- N operation. Then, the DFT can be used to decompose the N -block channels into independent channels whose capacities can be found easily. Using these ideas, we find the capacity region of a two-user Gaussian multiple-access channel in the following theorem.

Theorem 1

The capacity region of a two-user Gaussian multiple-access channel is

$$C = \bigcup_{\substack{\Sigma_1(\omega) \in \mathbb{R}^{p \times p}, \Sigma_2(\omega) \in \mathbb{R}^{q \times q} \\ \Sigma_i(\omega) \geq 0 \quad \forall \omega \in [0, \pi] \\ \frac{1}{2} \int_0^\pi \text{tr} \Sigma_i(\omega) d\omega \leq W_i, i=1,2.}} \quad (7)$$

$$\left\{ (R_1, R_2) : \begin{array}{l} R_1 \leq F(\Sigma_1(w), 0) \\ R_2 \leq F(0, \Sigma_2(w)) \\ R_1 + R_2 \leq F(\Sigma_1(w), \Sigma_2(w)) \end{array} \right\} \quad (7)$$

where

$$F(A, B) = \frac{1}{2\pi} \int_0^\pi \log \det [I + G(w)AG^*(w)R^{-1}(w) + H(w)BH^*(w)R^{-1}(w)] dw \quad (8)$$

A^* denotes the conjugate transpose of A and $G(w)$, $H(w)$ and $R(w)$ are the Fourier Transforms of \hat{G}_i , \hat{H}_i and \hat{R}_i , respectively.

Remark: It is easy to check that the above capacity region degenerates to the single-user multi-variate case obtained in [16] and the well known water-filling result in the single-user univariate case (e.g. [8]).

Corollary 1

If $p = q = 1$, the capacity of a two-user Gaussian multiple-access channel is

$$C = \bigcup_{\substack{S_1(w), S_2(w) \in \mathbb{R} \\ S_i(w) \geq 0 \quad \forall w \in [0, \pi] \\ \frac{1}{\pi} \int_0^\pi S_i(w) dw \leq W_i, \quad i=1,2.}} \left\{ (R_1, R_2) : \begin{array}{l} R_1 \leq F(S_1(w), 0) \\ R_2 \leq F(0, S_2(w)) \\ R_1 + R_2 \leq F(S_1(w), S_2(w)) \end{array} \right\} \quad (9)$$

where

$$F(A, B) = \frac{1}{2\pi} \int_0^\pi \log [1 + AT_1(w) + BT_2(w) + AB(T_1(w)T_2(w) - |T_{12}(w)|^2)] dw \quad (10)$$

$T_1(w) = G^*(w)R^{-1}(w)G(w)$, $T_2(w) = H^*(w)R^{-1}(w)H(w)$ and $T_{12}(w) = G^*(w)R^{-1}(w)H(w)$.

III Optimal Input Power Spectral Densities

In this section, we consider the multiple-access channel in the univariate case (i.e. $p = q = r = 1$), and give a geometric characterization of the optimal input power spectral densities of the users. It turns out that every boundary point of the capacity region can be obtained through the idea of water-filling argument and successive decoding.

Theorem 2

If $p = q = r = 1$, the capacity of a two-user Gaussian multiple-access channel is

$$C = \{(R_1, R_2) :$$

$$\begin{array}{l} \forall \theta \in [0, \frac{\pi}{4}] : R_1 \sin \theta + R_2 \cos \theta \leq \\ F(S_1(\theta, w), S_2(\theta, w)) \sin \theta + F(0, S_2(\theta, w)) (\cos \theta - \sin \theta) \\ \forall \theta \in [\frac{\pi}{4}, \frac{\pi}{2}] : R_1 \sin \theta + R_2 \cos \theta \leq \\ F(S_1(\theta, w), 0) (\sin \theta - \cos \theta) + F(S_1(\theta, w), S_2(\theta, w)) \cos \theta \end{array} \quad (11)$$

where $T_1(w) = |G(w)|^2/R(w)$, $T_2(w) = |H(w)|^2/R(w)$, $f_1(w) = \sin \theta - b_1 T_1^{-1}(w)$, $f_2(w) = \cos \theta - b_2 T_2^{-1}(w)$,

$$F(A, B) = \frac{1}{2\pi} \int_0^\pi \log [1 + A \frac{T_1(w)}{b_1} + B \frac{T_2(w)}{b_2}] \quad (12)$$

and $b_1 > 0$, $b_2 > 0$, $S_1(\theta, w)$, $S_2(\theta, w)$ are the solutions of

$$\frac{1}{\pi} \int_0^\pi S_k(\theta, w) dw = b_k W_k \quad k = 1, 2. \quad (13)$$

$$\begin{aligned} S_1(\theta, w) + S_2(\theta, w) &= [f_1(w) + [f_2(w) - f_1(w)]^+]^+ \\ &= [f_2(w) + [f_1(w) - f_2(w)]^+]^+ \end{aligned} \quad (14)$$

$$\begin{cases} \text{if } \theta \in [0, \pi/4] : \\ S_1(\theta, w) = \left[f_1(w) - b_1 T_1^{-1}(w) \frac{[f_2(w) - f_1(w)]^+}{[b_2 T_2^{-1}(w) - b_1 T_1^{-1}(w)]^+} \right]^+ \\ \text{if } \theta \in [\pi/4, \pi/2] : \\ S_2(\theta, w) = \left[f_2(w) - b_2 T_2^{-1}(w) \frac{[f_1(w) - f_2(w)]^+}{[b_1 T_1^{-1}(w) - b_2 T_2^{-1}(w)]^+} \right]^+ \end{cases} \quad (15)$$

and whenever the situation 0/0 arises in (15), the corresponding power spectral density $S_k(w)$ can be anything between $[0, f_k(w)]$.

Remark: In order to understand the mechanics in obtaining the optimal power spectral densities in this multiple access channel, we need first to consider the single-user case. In the traditional water-filling argument, we plot the inverse of the square of the channel transfer function, $T^{-1}(w)$, and adjust the water level such that the total amount of water is equal to the allowed power, W . An equivalent procedure is to plot the curve $a - bT^{-1}(w)$ for some fixed $a > 0$, and adjust the positive parameter, b , such that the area under the curve is equal to bW . Then, the curve gives the optimal power spectral density scaled by b . Notice that different values of a gives the same graph up to a scaling factor once the value of b is determined correspondingly.

Using this graphical method, we extend the result to the two-user case. In the two-user case, we have two graphs, one for each user, and four parameters a_1 , a_2 , b_1 and b_2 . For each θ in (11), we set $a_1 = \sin \theta$, $a_2 = \cos \theta$ and put the curves, $f_1(w) = \sin \theta - b_1 T_1^{-1}(w)$ and $f_2(w) = \cos \theta - b_2 T_2^{-1}(w)$, together and graphically obtain the two curves in (14) and (15). Notice that the curve in (14) is the maximum of $f_1(w)$ and $f_2(w)$ while the curve in (15) can be obtained by, say $\theta \in [0, \pi/4]$, subtracting a scaled version of $[f_2(w) - f_1(w)]^+$ from $f_1(w)$. Next, we adjust b_1 and b_2 such that the areas under the curves in (14) and (15) are $b_1 W_1 + b_2 W_2$ and $b_1 W_1$ (if $\theta \in [0, \pi/4]$) or

$b_2 W_2$ (if $\theta \in [\pi/4, \pi/2]$). Then, the curve in (15) and the difference between the two curves in (14) and (15) give the users' optimal power spectral densities that maximize $R_1 \sin \theta + R_2 \cos \theta$.

In the single-user case, the two degrees of freedom in a and b correspond to the power, W , and the scaling factor of the graph. In the two-user case, there are four degrees of freedom: a_1, a_2 , (or, equivalently, $\bar{a} \triangleq \sqrt{a_1^2 + a_2^2}$, $\theta \triangleq \tan^{-1}(a_1/a_2)$), b_1 , and b_2 . The parameter \bar{a} corresponds to the scaling factor of the graph while the parameter θ determines the boundary point under consideration. Finally, the two degrees of freedom in b_1 and b_2 correspond to the power of the users, W_1 and W_2 . Given a single-user channel, each $(a, b) \in \mathbb{R}_+^2$ determines the optimal spectral density for the user with some power constraint W . Similarly, given a two-user channel, each $(a_1, b_1, a_2, b_2) \in \mathbb{R}_+^4$ determines the optimal spectral densities of the users with some power constraints, W_1 and W_2 , with respect to a boundary point.

Remark: The intuitive interpretation of the formulas involves two ideas: successive decoding and the water-filling argument, and is best understood by the following two conditions on the spectral densities, which give (14) and (15):

$$S_1(w) + S_2(w) = \max\{\sin \theta - b_1 T_1^{-1}(w), \cos \theta - b_2 T_2^{-1}(w), 0\} \quad (16)$$

$$\begin{cases} \text{if } \theta \in [0, \pi/4]: \\ S_1(w) = [\sin \theta - b_1(T_1^{-1}(w) + S_2(w) \frac{T_1^{-1}(w)}{b_2 T_2^{-1}(w)})]^+ \\ \text{if } \theta \in [\pi/4, \pi/2]: \\ S_2(w) = [\cos \theta - b_2(T_2^{-1}(w) + S_1(w) \frac{T_2^{-1}(w)}{b_1 T_1^{-1}(w)})]^+ \end{cases} \quad (17)$$

When $\theta \in [0, \pi/4]$, the system is biased towards user 2, and the decoder will decode the information of user 1, treating the information of user 2 as noise, and then subtract the reconstructed signal of user 1 from the received signal before decoding the information of user 2. This is Cover's successive decoding idea [17] that is to explain the capacity region of the classical Gaussian multiple-access channel. Since the information sent by user 1 (assuming that it is decoded correctly) does not affect user 2, the traditional water-filling argument can be applied to user 1, treating the information of user 2 as noise, as in (17) once the power spectral density of user 2 is obtained.

Although the signal sent by user 1 had been subtracted when decoding user 2, the optimal spectral density for user 2 should not be obtained by blindly applying the traditional water-filling argument. This is because the signal of user 2 will act as noise to user 1 and its effect on the rate of user 1 cannot be ignored. Therefore, we have to determine the power spectral densities for both users together.

It turns out that we should look at both channels at the same time and consider a virtual user with power con-

strained by $W_1 + W_2$. However, the rewards of sending over these channels are not the same, but scaled by $\sin \theta$ and $\cos \theta$, respectively. Equation (16) gives the optimal power spectral density obtained by plotting the curves, $f_1(w)$ and $f_2(w)$, together with $a_1 = \sin \theta$ and $a_2 = \cos \theta$ and picking the larger power spectral density for each w .

Remark: When $\theta = \pi/4$, the total capacity is under consideration and $f_1(w) - f_2(w) = b_2 T_2^{-1}(w) - b_1 T_1^{-1}(w)$. Then, it is clear that $S_k(w)$ is equal to either $f_k(w)$ or 0. Hence, as in the classical white Gaussian MAC without ISI, FDMA achieves the total capacity.

Remark: The result degenerates to the classical water-filling argument when the channel response of one of the users is 0. For example, if $T_2(w) = 0$, $T_2^{-1}(w) = \infty$ and we are only interested in the case when $\theta = 0$. In such case, equation (14) gives $S_1(w) = [f_1(w)]^+$, which is essentially the classical water-filling argument.

A special case of the above theorem where $T_1(w) = T_2(w)$ for all w has been considered before in ([14], see also [13]). This situation may happen if the signals of the users are superimposed before entering a single-input channel. It turns out that, the capacity region is a pentagon which can be shown easily using the Karhunen-Loève decomposition.

Corollary 2

If $T_1(w) = T_2(w) \triangleq T(w)$, the capacity region of a two-user Gaussian multiple-access channel is

$$C = \left\{ (R_1, R_2) : \begin{array}{l} R_1 \leq \frac{1}{2\pi} \int_0^\pi \log[\max(\theta_1 T(w), 1)] dw \\ R_2 \leq \frac{1}{2\pi} \int_0^\pi \log[\max(\theta_2 T(w), 1)] dw \\ R_1 + R_2 \leq \frac{1}{2\pi} \int_0^\pi \log[\max(\theta_{12} T(w), 1)] dw \end{array} \right\} \quad (18)$$

where

$$\frac{1}{\pi} \int_0^\pi \max(\theta_i - T^{-1}(w), 0) dw = W_i \quad i = 1, 2. \quad (19)$$

$$\frac{1}{\pi} \int_0^\pi \max(\theta_{12} - T^{-1}(w), 0) dw = W_1 + W_2 \quad (20)$$

To illustrate how these ideas work, we give four examples representing different levels of intersymbol interference.

Examples:

$$1. G(w) = \frac{1+0.1e^{-jw}}{\sqrt{1.01}}, H(w) = \frac{1+0.2e^{-jw}}{\sqrt{1.04}}$$

$$2. G(w) = \frac{1+0.8e^{-jw}}{\sqrt{1.64}}, H(w) = \frac{1+0.9e^{-jw}}{\sqrt{1.81}}$$

$$3. G(w) = \frac{1+0.1e^{-jw}}{\sqrt{1.01}}, H(w) = \frac{1-0.2e^{-jw}}{\sqrt{1.04}}$$

$$4. G(w) = \frac{1+0.8e^{-jw}}{\sqrt{1.64}}, H(w) = \frac{1-0.9e^{-jw}}{\sqrt{1.81}}$$

In all four examples, we assume that $W_1 = 3$, $W_2 = 4$, the white Gaussian noise has variance 1 and the impulse

responses of all channels are normalized. In Examples 1 and 3, intersymbol interference is mild while in Examples 2 and 4, intersymbol interference is much stronger. In Examples 1 and 2, the channels for both users are all low-pass while in Examples 3 and 4, one user has a low-pass channel and the other user has a high-pass channel. The capacity regions of the channels in Example 1 and 2 are shown in Figure 4 while those in Example 3 and 4 are shown in Figure 5. It is clear, from all four examples, that with the energy of the transfer functions fixed, intersymbol interference decreases the single-user capacity. However, the same is not necessarily true for the total capacity. When the channels are all low-pass, the total capacity decreases as intersymbol interference increases as shown in Figure 4. When the channels of the two users are of different types, one low-pass and one high-pass, the total capacity actually increases as intersymbol interference becomes stronger.

In the single-user ISI channel, we can obtain the power spectral density by an algorithm iterating on b until the area under $a - bT^{-1}(w)$ is equal to bW . In the two-user channel, we give a similar algorithm which has two levels of iteration: one on b_1 and the other on b_2 . First, we arbitrarily fix b_2 and plot $f_2(w)$ in Figure 6a. Then, we adjust b_1 and plot $f_1(w)$ such that the total shaded area is equal to $b_1W_1 + b_2W_2$. On the same graph, we construct the curve ABXC, shown in Figure 6b, by subtracting $f_2(w) - f_1(w)$, scaled by a function of $T_1(w)$ and $T_2(w)$, from $f_1(w)$. If the area under the curve ABXC is larger than b_1W_1 , we decrease the value of b_2 (thereby raising $f_2(w)$), otherwise we increase the value of b_2 . Repeating the same procedure until the area under the curve ABXC is close enough to b_1W_1 , we obtain the optimal power spectral densities of user 1 (the shaded area in Figure 6b) and user 2 (the difference between $f_2(w)$ and the curve ABXC.)

Notice that the curve ABXC in Figure 6b is constructed from (16) and (17). According to (16), WX is equal to $S_1(w) + S_2(w)$ while WY is equal to

$$S_1(w) + S_2(w)b_1T_1^{-1}(w)/(b_2T_2^{-1}(w)).$$

Hence, the ratio of XY to XZ is $b_1T_1^{-1}(w)/(b_2T_2^{-1}(w))$ to 1 and we have

$$XY = YZ \frac{b_1T_1^{-1}(w)}{b_2T_2^{-1}(w) - b_1T_1^{-1}(w)} \quad (21)$$

Using this relationship, we can construct the curve ABXC graphically to obtain the optimal power spectral densities for the users.

References

[1] C. E. Shannon, "A mathematical theory of communication I & II," *Bell System Technical Journal*, vol. 27, pp. 379-423, 623-656, July & October 1948.

- [2] R. Ahlswede, "Multi-way communication channels," in *Proceedings of 2nd International Symposium on Information Theory*, (Tsahkadsor, Armenia, USSR), pp. 23-52, September 1971.
- [3] H. Liao, "A coding theorem for multiple access communications," Presented at *International Symposium on Information Theory*, Asilomar, 1972.
- [4] R. Ahlswede, "The capacity of a channel with two senders and two receivers," *Annual Probability*, vol. 2, pp. 805-814, October 1974.
- [5] I. Csiszár and J. Körner, *Information Theory: Coding theorems for discrete memoryless systems*. London: Academic Press, INC., 1981.
- [6] J. Wolfowitz, *Coding Theorems of Information Theory*. New York: Springer, 3rd ed., 1978.
- [7] C. E. Shannon, "Communication in the presence of noise," *Proc. IRE*, vol. 37, pp. 10-21, January 1949.
- [8] R. G. Gallager, *Information theory and reliable communication*. New York: John Wiley & Son, 1968.
- [9] B. S. Tsybakov, "Capacity of a discrete-time Gaussian channel with a filter," *Probl. Peredach. Inform.*, vol. 6, pp. 78-82, July-September 1970.
- [10] R. G. Gray, "On the asymptotic eigenvalue distribution of Toeplitz matrices," *IEEE Transaction on Information Theory*, vol. IT-18, no. 6, pp. 267-271, November 1972.
- [11] S. Verdú, "Multiple-access channels with memory with and without frame synchronism," *IEEE Transaction on Information Theory*, vol. IT-35, no. 3, pp. 605-619, May 1989.
- [12] S. Verdú, "The capacity region of the symbol-asynchronous Gaussian multiple-access channel," *IEEE Transaction on Information Theory*, vol. IT-35, no. 4, pp. 733-751, July 1989.
- [13] C. W. Keilers, *The capacity of the spectral Gaussian multiple-access channel*. PhD thesis, Stanford University, May 1976.
- [14] C. M. Zeng, N. He, and F. Kuhlmann, "Capacity region of a waveform Gaussian multiple-access channel," in *Book of Abstracts of the 1990 International Symposium on Information Theory*, (San Diego, CA), p. 93, January 1990.
- [15] W. Hirt and J. L. Massey, "Capacity of the discrete-time Gaussian channel with intersymbol interference," *IEEE Transaction on Information Theory*, vol. IT-34, no. 3, pp. 380-388, May 1988.

[16] L. H. Brandenburg and A. D. Wyner, "Capacity of the Gaussian channel with memory: the multivariate case," *Bell System Technical Journal*, vol. 53, no. 5, pp. 745-778, May-June 1974.

[17] T. Cover, *Some advances in broadcast channels*, vol. 4, pp. 229-260. New York: Academic Press, 1975.

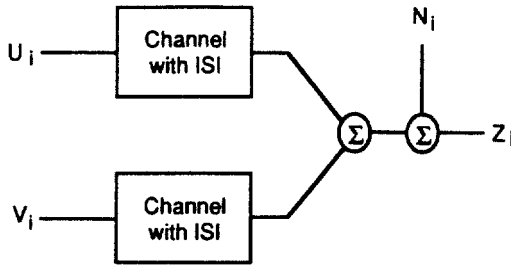


Figure 1. Multi-user Gaussian Channel with ISI

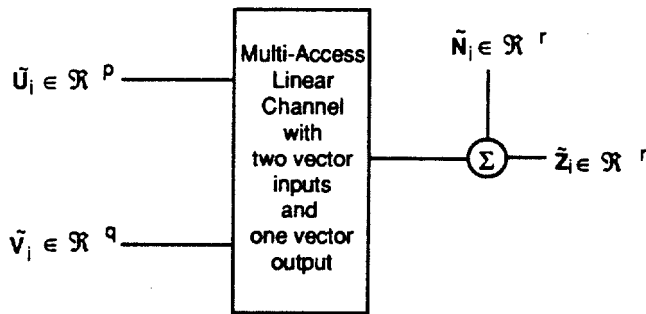


Figure 2. Multi-user Gaussian Linear Vector Channel

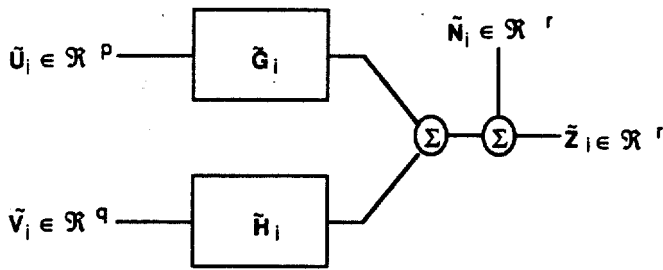


Figure 3. Equivalent Model for Multi-user Gaussian Linear Vector Channel

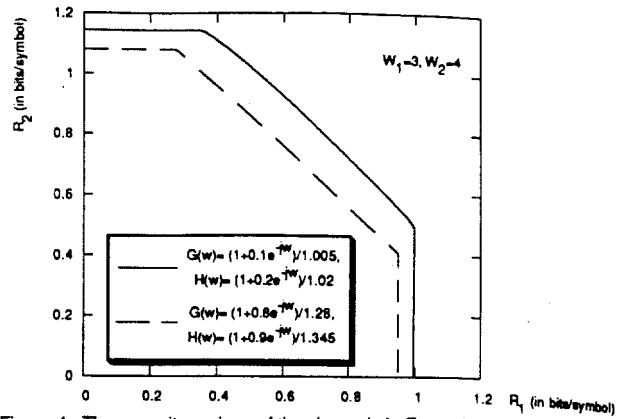


Figure 4. The capacity regions of the channels in Examples 1 & 2

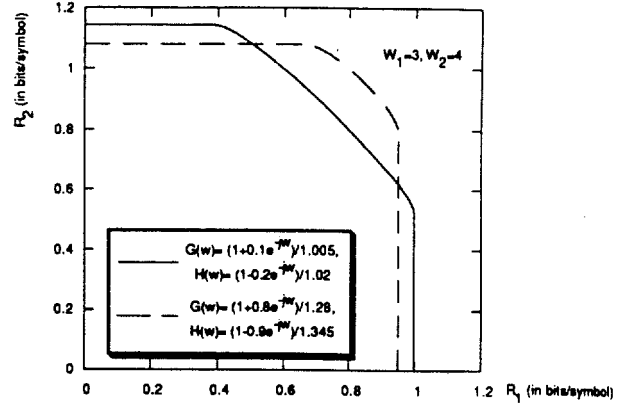


Figure 5. The capacity regions of the channels in Examples 3 & 4

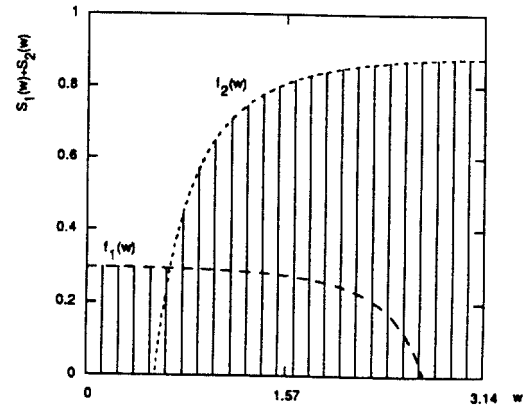


Figure 6a. Sum of the users' Optimal Power Spectral Densities in Example 4

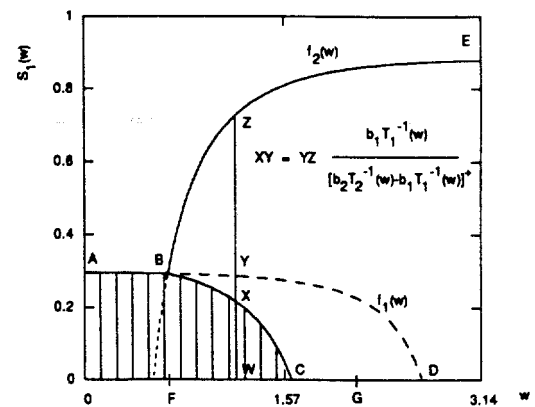


Figure 6b. Optimal Power Spectral Densities of the users in Example 4